

My, how you've grown:
A practical guide to modeling size transitions
for Integral Projection Model (IPM) applications

Tom E.X. Miller^{*a} and Stephen P. Ellner^b

^aDepartment of BioSciences, Rice University, Houston TX

^bDepartment of Ecology & Evolutionary Biology, Cornell University, Ithaca NY

Submitted to: *Ecology* (Statistical Report)

Keywords: demography; growth; integral projection model; kurtosis; skewness

Open Research Statement: Data are already published and publicly available, with those items properly cited in this submission. Three data sets are cited as data packages (Ochocki *et al.*, 2023; Winfield *et al.*, 2013b; Miller, 2020). Two other data sets are available in our Github repo, which also includes all of our code. The repo will be archived in a Zenodo package, with the DOI included at the end of the article, upon publication. During peer review, our data and code are available at https://github.com/texmiller/IPM_size_transitions.

*Corresponding author. Department of BioSciences, Rice University, Houston, TX 77005-1827. Email: tom.miller@rice.edu
Phone: 713-348-4218

¹ **Abstract**

² Integral Projection Models (IPMs) are widely used for studying continuously size-structured popula-
³ tions. IPMs require a growth sub-model that describes the probability of future size conditional on current size
⁴ and any covariates. Most IPM studies assume that this distribution is Gaussian, despite calls for non-Gaussian
⁵ models that accommodate skewness and excess kurtosis. We provide a general workflow for accommodating
⁶ non-Gaussian growth patterns while retaining important covariates and random effects. Our approach empha-
⁷ sizes visual diagnostics from pilot Gaussian models and quantile-based metrics of skewness and kurtosis that
⁸ guide selection of a non-Gaussian alternative, if necessary. Across five case studies, skewness and excess kur-
⁹ tosis were common features of growth data and non-Gaussian models consistently generated simulated data
¹⁰ that were more consistent with real data than pilot Gaussian models. However, effects of “improved” growth
¹¹ modeling on IPM results were moderate to weak, and differed in direction or magnitude between different out-
¹² puts from the same model. Using tools not available when IPMs were first developed, it is now possible to fit
¹³ non-Gaussian models to growth data without sacrificing ecological complexity. Doing so, as guided by careful
¹⁴ interrogation of the data, will result in models that better represent the populations for which they are intended.

15 **1 Introduction**

16 Structured demographic models – matrix and integral projection models (MPMs and IPMs) – are powerful
17 tools for data-driven modeling of population and community dynamics. In contrast to MPMs for populations
18 with discrete structure (life stage, age class, etc.), IPMs (Easterling *et al.*, 2000) accommodate populations
19 structured by continuous state variables, most commonly size. A related innovation of the IPM framework
20 is its emphasis on regression-based modeling for parameter estimation, which often carries important
21 advantages for making the most of hard-won data (Ellner *et al.*, 2022).

22 A standard workflow allows ecologists to assemble an IPM from data using familiar regression
23 tools to describe growth, survival, reproduction, and other demographic transitions as functions of size
24 (Coulson, 2012; Ellner *et al.*, 2016). The relative ease of regression analyses, accommodating covariates
25 (e.g., environmental factors, experimental treatments) and complex variance structures (e.g., random effects,
26 correlated errors), has facilitated a growing IPM literature that examines how biotic or abiotic factors affect
27 population dynamics (e.g., Louthan *et al.*, 2022; Ozgul *et al.*, 2010) and explores the consequences of
28 demographic heterogeneity associated with spatial, temporal, and individual variation (e.g., Compagnoni *et al.*,
29 2016; Crone, 2016; Plard *et al.*, 2018). The vital rate regressions (or “sub-models”) are the bridge between
30 the individual-level data and the population-level model and its predictions; it is important to get those right.

31 Compared to other vital rates, growth is special. The survival and reproduction sub-models only
32 need to provide a single predicted value as functions of size (we use “size” as the name for whatever
33 continuous variable defines the population structure). But the growth model must specify the full probability
34 distribution of subsequent size conditional on initial size, defining the growth ‘kernel’ $G(z', z)$ that gives the
35 probability density of future size z' at time $t+1$ conditional on current size z at time t . Whenever survival
36 and reproduction are size-dependent, the entire distribution of size transitions can strongly influence IPM
37 predictions because it governs how frequently size changes are much greater or much lower than average.

38 Easterling et al. 2000 provided the original template for modeling size transitions in IPMs. They
39 first tried simple linear regression, assuming Normally distributed size changes with constant variance.
40 Because the residuals from this regression exhibited non-constant variance, they used a two-step approach
41 to estimate the size-dependence in mean squared residuals (better options soon became available, such
42 as the `lme` function in R). However, even after accounting for non-constant variance, growth data may
43 still be non-Normal. Size transitions are often skewed such that large decreases are more common than
44 large increases (Peterson *et al.*, 2019; Salguero-Gómez & Casper, 2010), or vice versa (Stubberud *et al.*,
45 2019). Size transitions may also exhibit excess kurtosis (“fat tails”), where extreme growth or shrinkage
46 is more common than predicted by the tails of the Normal distribution (Hérault *et al.*, 2011).

47 The observation that the Normal (or Gaussian) distribution may poorly describe size transitions in real
48 organisms has been made before, and several studies have emphasized that alternative distributions should be
49 explored (Easterling *et al.*, 2000; Peterson *et al.*, 2019; Rees *et al.*, 2014; Williams *et al.*, 2012). For example,
50 Peterson et al. 2019 showed that skewness in size transitions could be modeled through beta regression
51 on transformed data (for reasons we describe below, this approach also has some drawbacks), or by fitting
52 a skewed Normal distribution. They showed that incorporating skew could have important consequences for
53 model-based inferences, and concluded that “testing of alternative distributions for growth... [should] become
54 standard in the construction of size-structured population models.” Nonetheless, default use of Gaussian
55 growth distributions (often with non-constant variance) remains the standard practice. The general state-of-
56 the-art in the literature appears to remain where it was 20 or so years ago, using the default Gaussian model
57 without examining critically whether or not it actually describes the data well. We are guilty of this, ourselves.

58 The persistence of Gaussian growth models is understandable. Popular packages such as `lme4` (Bates
59 *et al.*, 2015), `mgcv` (Wood, 2017), and `MCMCglmm` (Hadfield *et al.*, 2010) make it easy to fit growth
60 models with potentially complex fixed- and random-effect structures, but the possible distributions of
61 continuous responses are limited, and default to Gaussian. Abandoning these convenient tools for the sake

62 of more flexible growth modeling means, it may seem, sacrificing the flexibility to model diverse sources
63 of demographic variation, some of which may be the motivation driving the study in the first place.

64 Our goal here is to present and illustrate a practical “recipe” that moves growth modeling past the
65 standards set over 20 years ago. Using software tools that are now readily accessible, ecologists can escape
66 the apparent trade-off between realistically modeling non-Gaussian size transitions and flexibly including
67 multiple covariates and random effects.¹ As with any recipe, users may need to make substitutions or add
68 ingredients to suit their needs. We emphasize graphical diagnostics for developing and evaluating growth
69 models, rather than a process centered on statistical tests or model selection. Through empirical case studies
70 we demonstrate how tools that were nonexistent or not readily available when IPMs first came into use
71 now make it straightforward and relatively easy to identify when the default model is a poor fit to the
72 data, and to then choose and fit a better growth model that is no harder to use in practice. We illustrate
73 our approach by revisiting three published case studies (and three additional case studies in the Supporting
74 Information), including examples from our own previous work. In each case, the Gaussian assumption does
75 not stand up to close scrutiny. We illustrate how we could have done better, and the consequences of “doing
76 better” for our ecological inferences. All analyses were carried out in R (R Core Team, 2022) version 4.0
77 or higher and may be reproduced from publicly available code and data (see *Data Availability Statement*).

78 **2 Flexible growth modeling**

79 The modeling process that we suggest runs as follows (Fig. 1):

80 **1. Fit a “pilot” model assuming a Gaussian distribution, but allowing for non-constant variance.** This
81 step is familiar to most IPM users, as it is the start and end of the standard approach. It may include model
82 selection to identify which treatment effects or environmental drivers affect the mean and/or variance of future
83 size. Non-constant variance is often fitted in a two-stage process, first fitting mean growth assuming constant

¹Our statements about software availability are based on what current software reliably delivers in our personal experience, not on what they promise.

84 variance, then doing a regression relating the squared residuals to initial size or the fitted mean of subsequent
85 size. Fitting mean and variance simultaneously as functions of initial size, as can be done with R packages
86 **mgev** and **nmle**, is advantageous when possible because incorrectly assuming constant variance can affect
87 model selection for the mean. We illustrate both one-step and two-step approaches in the case studies below.

88 Allowing non-constant variance removes the need for transforming the data to stabilize growth variance.
89 Transformation may still be useful if it does not create new problems such as making some state-fate
90 relationships highly nonlinear. In particular, log-transformation often reduces or eliminates heteroskedasticity
91 in growth data (Ellner *et al.*, 2016) and also helps avoid eviction at small sizes (Williams *et al.*, 2012).

92 The fitted mean and variance functions should be checked before going any further. If they are
93 perfectly correct, standardized residuals (residuals scaled by the standard deviation) will have zero mean
94 and unit variance overall, and will exhibit no trends in mean or variance with initial size or fitted mean
95 value. However, estimates of the mean and variance functions are somewhat smoothed because of the
96 inescapable bias-variance tradeoff, so scaled residuals will retain some variation in location and scale. Given
97 enough data, statistical tests will detect that variation. So instead, we take for granted the presence of trends
98 and assess their importance by fitting nonparametric spline regression models for residuals (trend in mean)
99 and absolute residuals (trend in variance) as a function of initial size or fitted value. The mean and variance
100 functions can be accepted if the regression curves for the scaled residuals are nearly flat.

101 **2. Use graphical diagnostics to identify if and how the standardized residuals deviate from Gaussian,**
102 **and to choose a more appropriate distribution.** If the Gaussian growth model is valid, the standardized
103 residuals should be Gaussian with zero skewness or excess kurtosis. Growth data may deviate from this
104 in many ways, and the nature of the deviations can guide the search for a better distribution. Tests such as
105 the D'Agostino test of skewness (D'Agostino, 1970) and the Anscombe-Glynn test of kurtosis (Anscombe
106 & Glynn, 1983) can be used to diagnose whether the standardized residuals, in aggregate, deviate from

107 normality (Komsta & Novomestky, 2015). However, the aggregate distribution may be misleading if
108 skewness or kurtosis vary with size or other covariates. Skewness changing from positive at small sizes to
109 negative at large sizes might produce zero overall skewness, but really requires a distribution that can allow
110 both positive and negative skew, such as the skewed Normal or Johnson S_U distributions. Alternatively,
111 growth data may exhibit leptokurtosis (in which case the t distribution may be a good choice) or may
112 shift from platykurtosis to leptokurtosis depending on initial size (in which case the power exponential
113 distribution may be a good choice). It is therefore essential to visualize trends in distribution properties
114 with respect to either initial size, or expected future size for models with multiple covariates. Fig. 1 includes
115 guidance on how the skew and kurtosis properties of the standardized residuals suggest options for an
116 appropriate growth distribution. In our case studies we exploit the many distributions in the **gamlss** R
117 package (Stasinopoulos *et al.*, 2007), but other distribution families can be used.

118 **3. Refit the growth model using the chosen distribution.** In models with multiple covariates and/or ran-
119 dom effects, each potentially affecting several distribution parameters, “refit the model” could entail a massive
120 model selection process to identify the “best” non-Gaussian model. With so many options, model uncertainty
121 may be overwhelming and over-fitting becomes a significant risk even when precautions against it are taken.

122 We therefore argue for adopting a more modest goal: remedy the defects evident in the standardized
123 residuals of the Gaussian model. This recommendation is based on the finding that parameter estimation
124 using Gaussian regression models is generally robust to deviations from normality of the residuals
125 (Schielzeth *et al.*, 2020). That is, the fitted mean of the Gaussian model (as a function of covariates) is
126 probably a very good approximation for the fitted mean in the corresponding non-Gaussian model — and
127 if it is not, the next step in the modeling process will catch that. The functional forms for skew and kurtosis
128 of the non-Gaussian model can be guided by the qualitative features of the graphical diagnostics (e.g.,

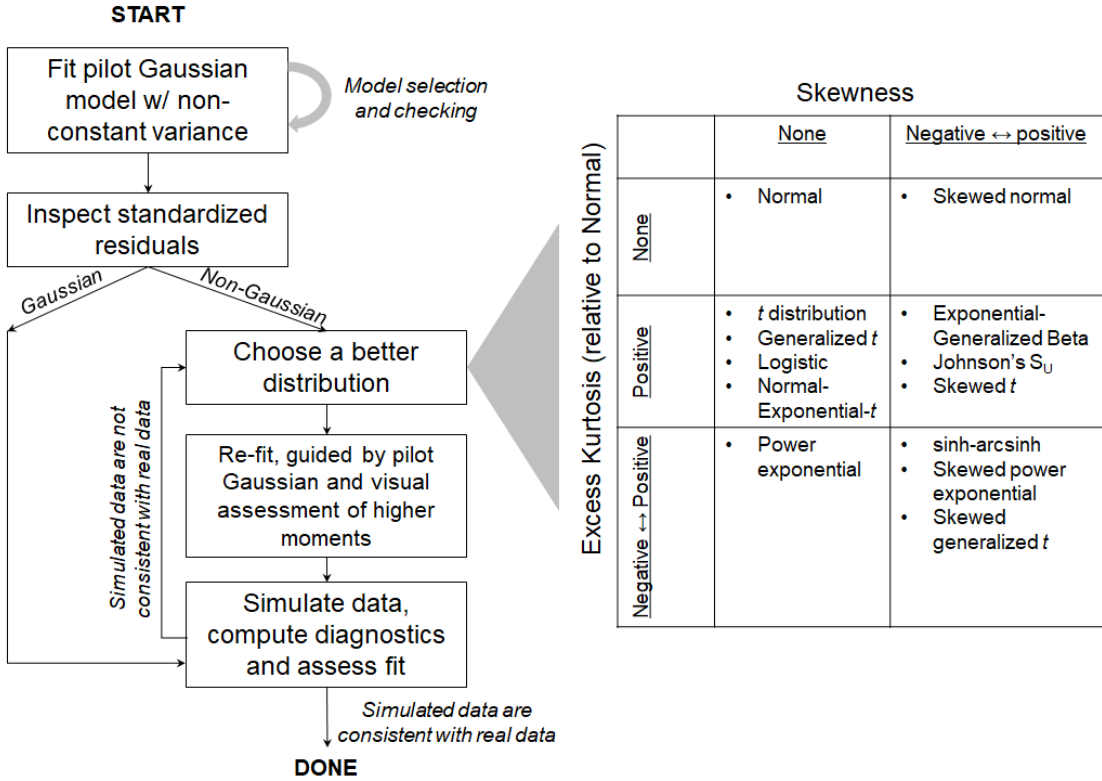


Figure 1: Recommended steps in growth modeling (left) and guide to common non-Gaussian distributions of size x for $x \in \mathbb{R}$ that can accommodate different combinations of skewness and kurtosis (right). All of these distributions (often including multiple versions or parameterizations of each) are available in the R package **gamlss.dist**, except for the skewed generalized *t*, which is available in the package **sgt** (Davis, 2015).

- 129 that skewness switches from positive to negative with increasing size). As we demonstrate below, the
 130 mean and standard deviation functions can often be carried over exactly from the pilot Gaussian model.
 131 **4. Evaluate the final growth model through graphical diagnostics comparing simulated and real**
 132 **growth data.** A good model will generate simulated data that look like the real data. Again, it is important
 133 to inspect the properties of simulated data as a function of initial size, fitted mean, or other covariates rather
 134 than examining the aggregate distribution. We again suggest below graphical diagnostics, based mainly
 135 on quantiles, that can be used to compare simulated with real growth data. If the simulated data do not
 136 correspond well with the real data, alternative or more flexible distribution families should be considered,
 137 or more complex functions relating distribution parameters to size and other covariates.

¹³⁸ **3 How should skewness and kurtosis be measured?**

¹³⁹ Non-Gaussian growth modeling requires scrutinizing the skewness and kurtosis of standardized residuals,
¹⁴⁰ so measurement of these properties warrants attention. The standard measures are based on the third and
¹⁴¹ fourth central moments, respectively, of the distribution: skewness = m_3/σ^3 , excess kurtosis = $m_4/\sigma^4 - 3$
¹⁴² where $m_k = \mathbb{E}(X - \bar{X})^k$ is the k^{th} central moment of a random variable X and σ^2 is the variance (second
¹⁴³ central moment). A Gaussian distribution has zero skewness and zero excess kurtosis.

¹⁴⁴ The standard measures are simple and easy to use, but they have poor sampling properties. Because
¹⁴⁵ the measures involve high powers of data values, a few outliers can produce very inaccurate estimates.
¹⁴⁶ Figure 2 shows a simulated example, where the underlying data are samples of 200 values from a t
¹⁴⁷ distribution with 8 degrees of freedom, repeated 5000 times; the true skew is 0, and the true excess kurtosis
¹⁴⁸ is 1.5. The distance between the largest and smallest estimates (indicated by the dotted red vertical lines),
¹⁴⁹ relative to the distance between the 5th and 95th percentiles, shows the broad extent of extreme values
¹⁵⁰ that can occur even with a large sample, especially for kurtosis.

¹⁵¹ We therefore recommend nonparametric (NP) measures of skewness and kurtosis that are based on
¹⁵² quantiles and thus are less sensitive to a few extreme values. Let q_α denote the α quantile of a distribution
¹⁵³ or sample (e.g., $q_{0.05}$ is the 5th percentile). For any $0 < \alpha < 0.5$, a quantile-based measure of skewness
¹⁵⁴ is given by (McGillivray, 1986)

$$\text{NP Skewness} = \frac{q_\alpha + q_{1-\alpha} - 2q_{0.5}}{q_{1-\alpha} - q_\alpha}. \quad (1)$$

¹⁵⁵ NP Skewness measures the asymmetry between the tails of the distribution above and below the median.
¹⁵⁶ The size of the upper tail can be measured (for any $0 < \alpha < 0.5$) by $\tau_U = q_{1-\alpha} - q_{0.5}$; for $\alpha = 0.05$ this
¹⁵⁷ is the difference between the 95th percentile and the median. The lower tail size is $\tau_L = q_{0.5} - q_\alpha$. The

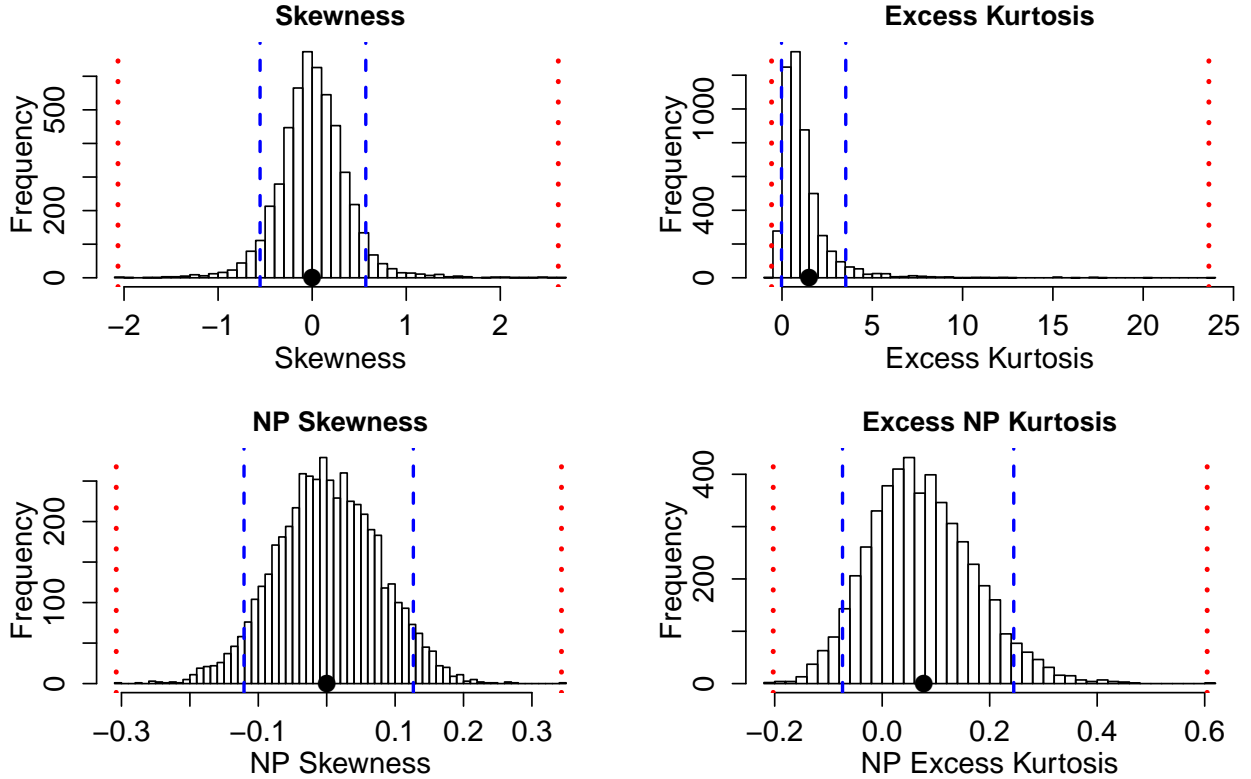


Figure 2: Histograms of skewness and kurtosis estimates using moment-based definitions (top two panels), compared with the nonparametric measures based on quantiles (bottom two panels). Note the very large differences in scale. Histograms are based on 5000 replicate draws of a sample of 200 independent values, from a t distribution with 8 degrees of freedom. Dotted red vertical lines mark the minimum and maximum of sample estimates, and dashed blue lines show the 5th and 95th percentiles. The true value is indicated by a black dot on the x -axis. Figure drawn by script `NPmoments.R`

159 definition above is equivalent to

$$160 \quad \text{NP Skewness} = \frac{\tau_U - \tau_L}{(\tau_U + \tau_L)}. \quad (2)$$

161 An NP Skewness of ± 0.2 says that the difference in tail sizes is 20% of their total. The range of possible
 162 values is -1 to 1. Both $\alpha=0.25$ (sometimes called “Kelly’s skewness”) and $\alpha=0.1$ (“Bowley’s skewness”)
 163 are common choices. We used $\alpha=0.1$.

164 An analogous quantile-based measure of kurtosis (Jones *et al.*, 2011) is

$$165 \quad \text{NP Kurtosis} = \frac{q_{1-\alpha} - q_\alpha}{q_{0.75} - q_{0.25}}. \quad (3)$$

166 For $\alpha=0.05$, NP Kurtosis is the difference between the 95th and 5th percentiles, relative to the interquartile
 167 range. To facilitate interpretation, we scale NP Kurtosis relative to its value for Gaussian distribution, and
 168 subtract 1 so that the value for a Gaussian is zero. We call this “NP Excess Kurtosis”. A value of ± 0.2
 169 means that the tails are on average 20% heavier than those of a Gaussian with the same interquartile range.
 170 We calculate NP Kurtosis using $\alpha=0.05$, to focus on the tail edges, but again this is somewhat arbitrary.

171 Figure 2C,D illustrate how, applied to the same simulated samples, the nonparametric measures
 172 produce a smaller fraction of highly inaccurate estimates caused by a few extreme values. Also note that,
 173 in contrast to the moment-based measures, numerically small values of the nonparametric measures (e.g., 0.1
 174 or 0.2) should not be disregarded, because both measures are scaled so that a value of 1 indicates extremely
 175 large departures from a Gaussian distribution.

176 Using quantile-based measures carries the added value that quantile regression can be used to estimate
 177 how they vary with initial size or expected future size. In the examples below, we use the **qgam** package
 178 (Fasiolo *et al.*, 2020) to fit spline quantile regression models, which accommodate nonlinear size-dependence
 179 in skewness and kurtosis. One risk of spline regression is that fitted quantiles may be excessively “wiggly”
 180 without constraints on their complexity; with realistic amounts of data, we can hope to estimate broad trends
 181 in distribution shape, but not fine-scale variation. In the examples below, we limit complexity by fitting
 182 splines with $k=4$ basis functions unless otherwise noted. Parametric quantile regression is also an option.

183 For consistency we also use quantile-based measures of mean and standard deviation when comparing
 184 real and simulated data, and use quantile regression to visualize their trends. Specifically, following Wan
 185 *et al.* (2014),

$$186 \text{NP Mean} = \frac{q_{0.25} + q_{0.5} + q_{0.75}}{3}, \quad \text{NP SD} = \frac{q_{0.75} - q_{0.25}}{1.35}. \quad (4)$$

187 **4 Case study: lichen, *Vulpicida pinastri***

188 We begin with a simple example where current size is the only predictor of future size. Growth data for
189 the epiphytic lichen *Vulpicida pinastri* were analyzed first by Shriver et al. 2012 and again by Peterson
190 et al. 2019 in their study of skewed growth distributions. We therefore had an *a priori* expectation of
191 deviation from normality. The data set includes 1,542 inter-annual transitions in thallus area (cm^2) observed
192 from 2004 to 2009 in Kennicott Valley, AK. Shriver et al. 2012 used a mixture distribution that separated
193 “normal growth or shrinkage” from “extreme shrinkage”. We aimed to fit a single growth model that could
194 realistically accommodate both types of size transition without requiring *ad hoc* decisions about which
195 observations of shrinkage were “extreme” or not.

196 With initial size as the only predictor, a convenient way to fit a Gaussian model with nonconstant
197 variance is the `gam` function in **mgcv** library (Wood, 2017) using the `gaulss` family. Following a bit
198 of model selection, we fit the mean and standard deviation of future size as second-order polynomials
199 of current size², then calculated the scaled residuals from the fitted mean and standard deviation. Here,
200 the first argument to `gam()` is a two-element list that defines the linear predictors for mean and sd:

```
201 # d is the data frame; t0,t1 are initial & final thallus area, respectively  
202 fitGAU <- gam(list(t1~t0 + I(t0^2), ~t0 + I(t0^2)), data=d, family=gaulss())  
203 d$fitted_mean = predict(fitGAU,type="response") [,1]  
204 d$fitted_sd <- 1/predict(fitGAU,type="response") [,2]  
205 d$scaledResids=residuals(fitGAU,type="response")/d$fitted_sd
```

206 The data and fitted mean and standard deviation are shown in Fig. 3A, and the corresponding diagnostic
207 plots are in Fig. 4A,B. Our diagnostic plots are similar to plots made by R’s `plot.lm` function, except
208 that we use spline regression to allow data-driven choice of curve smoothness, and use absolute residuals

²`gam()` is most commonly used to fit smooth splines (`s()`) for predictor variables, but it can also fit simpler, parametric regressions.

209 (rather than their square roots) so that the standard deviation of the regression curve is on the same scale
210 as the residuals. The spline curves are not exactly flat – their standard deviations, given above each panel,
211 are positive – but the trends are much too small to be worth fixing.

212 Quantile regression on the scaled residuals generates the skewness and kurtosis diagnostics shown
213 in Fig. 3B. As expected based on previous analyses, the graphical analysis of the standardized residuals
214 indicates negative skew, especially at larger sizes (Fig. 3B). We also find positive excess kurtosis for all sizes.

215 We turned to the Johnson's *S-U* (JSU) distribution for improvement. The JSU is a four-parameter
216 leptokurtic distribution allowing positive or negative skew, with the convenient property that its location
217 and scale parameters `mu` and `sigma` are the mean and standard deviation, respectively, which greatly
218 facilitates the transition from a pilot Gaussian model. JSU is not available in any standard linear or additive
219 modeling packages, to our knowledge. But that is not a barrier because we can write a likelihood function
220 using the `dJSU()` function in the **gamlss.dist** package. Following the best-fit Gaussian model, we defined
221 `mu` and `sigma` of the JSU as quadratic polynomials of initial size and, based on Fig. 3B) we define the
222 skewness parameter `nu` as a linear function of size and kurtosis parameter `tau` as a positive constant.
223 The likelihood function therefore has nine parameters to estimate. We fit the model using the **maxLik**
224 package³ with starting coefficient values for `mu` and `sigma` based on the pilot Gaussian model:

```
225 ## define function that returns the JSU negative log-likelihood  
226 LogLikJSU=function(pars){  
227   dJSU(t1, mu=pars[1]+pars[2]*t0+pars[3]*t0^2,  
228         sigma=exp(pars[4]+pars[5]*t0+pars[6]*t0^2),  
229         nu = pars[7]+pars[8]*t0, tau = exp(pars[9]), log=TRUE)  
230 }
```

³We chose **maxLik** because it offers the BHHH optimization method, which works well for non-Gaussian likelihoods in our experience.

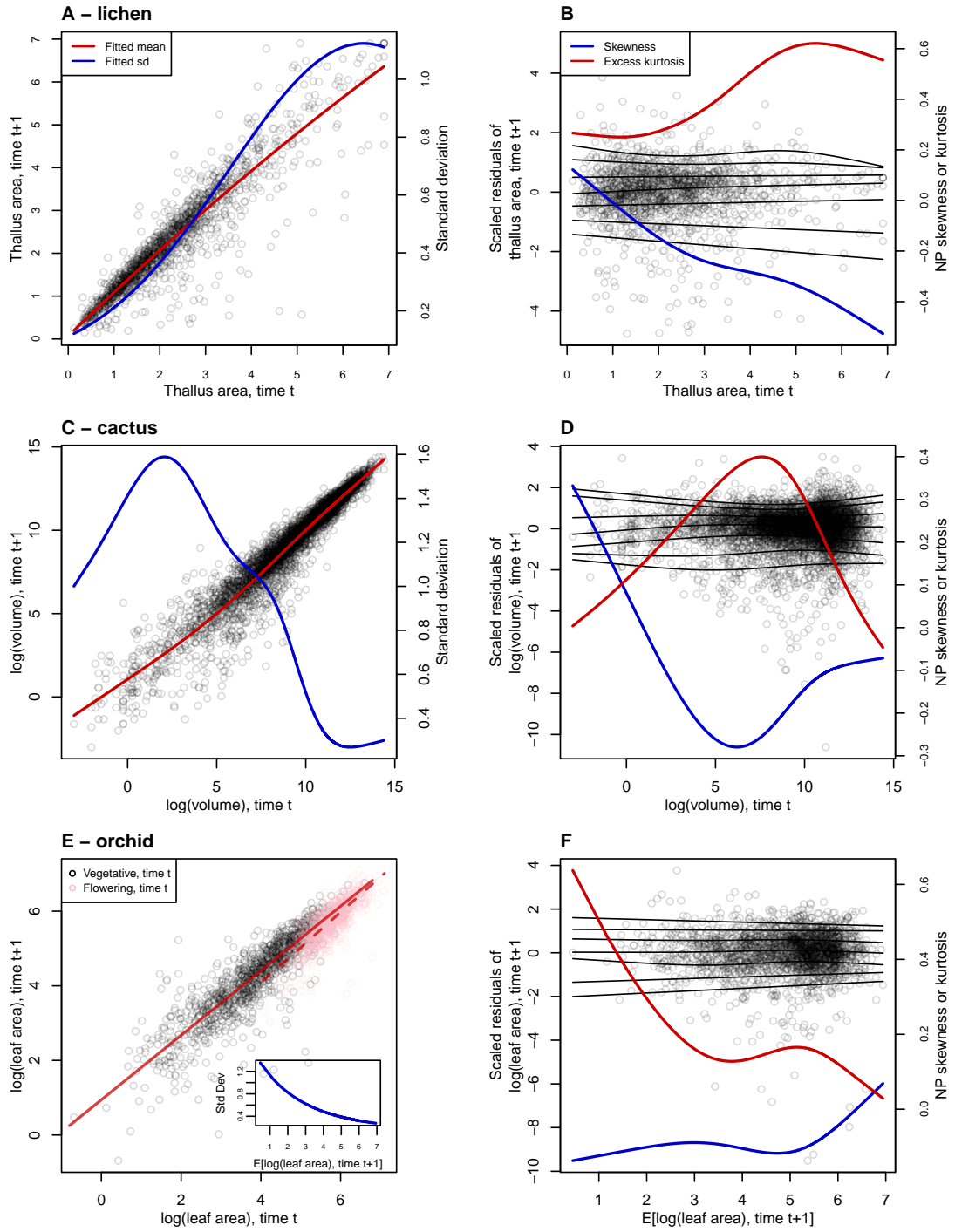


Figure 3: Best Gaussian models and diagnostics of standardized residuals for lichen (*Vulpicida pinastri*) **A,B**, cactus (*Cylindriopuntia imbricata*) **C,D**, and orchid (*Orchis purpurea*) **E,F** case studies. **A,C**, fitted mean (red) and standard deviation (blue) of size at time $t+1$ conditional on initial size at time t . **E**, fitted means for plants that were vegetative (solid line) or flowering (dashed line) at the start of the census interval and standard deviation as a function of the fitted mean (inset). **B,D,F** Quantile regressions of scaled residuals (lines show 5%, 10%, 25%, 50%, 75%, 90%, and 95% quantiles) and non-parametric measures of skewness (blue) and excess kurtosis (red) derived from them. In **B,D** scaled residuals are shown with respect to initial size and in **F** they are shown with respect to fitted values. Figure made by script `crosspp_growth.R`.

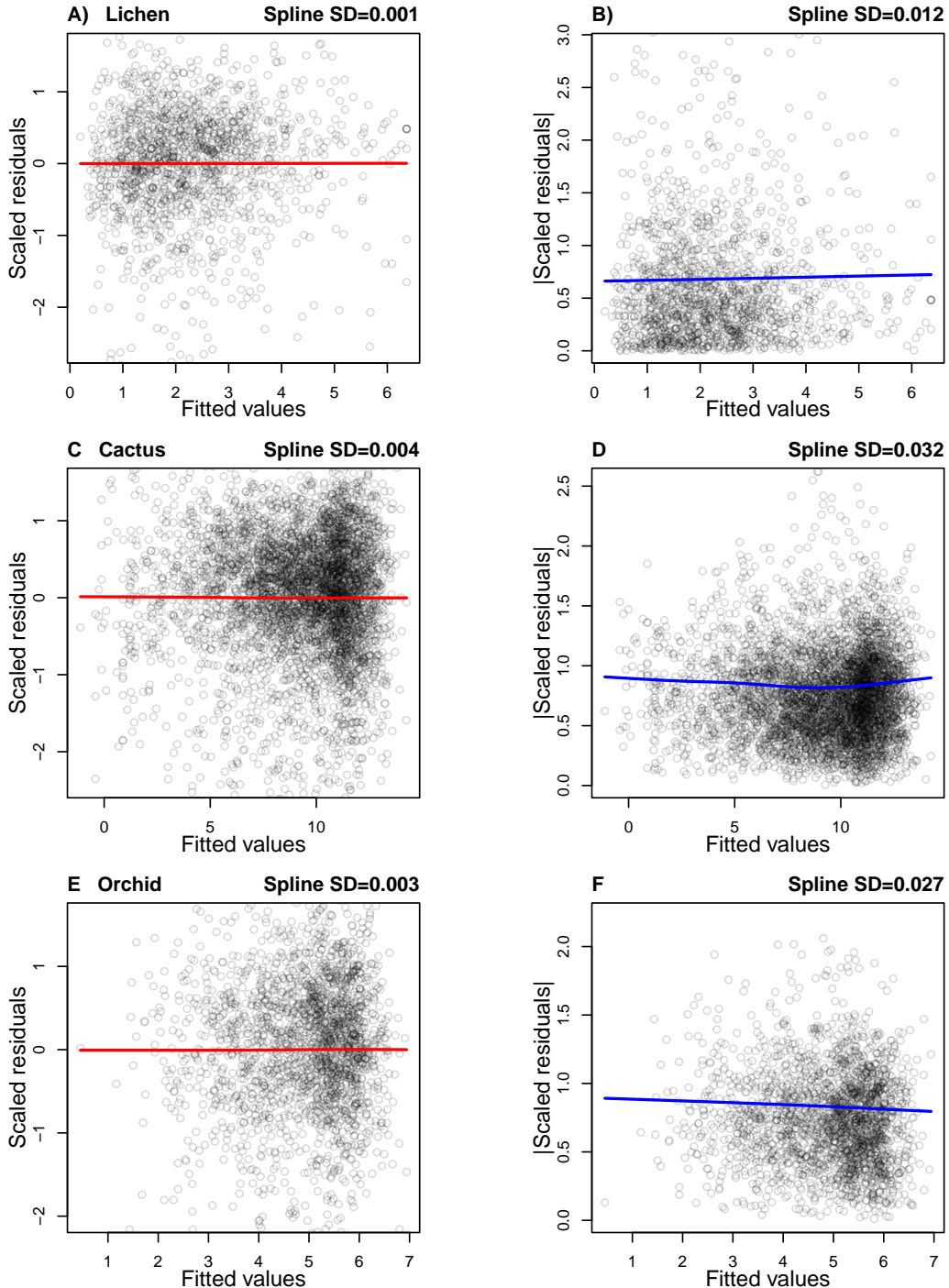


Figure 4: Diagnostic plot for trends in the mean (left column) or variance (right column) of scaled residuals from a pilot Gaussian model, for the lichen (*Vulpicida pinastri*) **A,B**, cactus *Cylindropuntia imbricata* **C,D**, and orchid *Orchis purpurea* **E,F** case studies. In **A,C,E** the standardized residuals are plotted, and in **B,D,F** the absolute values of standardized residuals, as functions of fitted mean subsequent size values. The solid curves are cubic splines (R function `smooth.spline`) fitted by generalized cross-validation with a modest over-penalization of model degrees of freedom to prevent overfitting (penalty=1.4 as recommended by Gu (2013)). The numbers appearing above each panel are the standard deviation of the values on the spline regression curve, evaluated at all of the fitted values. Figure made by script `crosspp_diagnose_pilot.R`.

```

231 ## starting parameter values
232 p0<-c(coef(fitGAU)[1:6],0,0,0)
233 ## fit with maxlik, adding some noise to starting values
234 outJSU=maxLik(logLik=LogLikJSU,start=p0*exp(0.2*rnorm(length(p0))),  

235 method="BHHH",control=list(iterlim=5000,printLevel=2),finalHessian=FALSE);

```

236 Simulating data from the fitted JSU model indicates a compelling improvement over the best Gaussian
237 model, not only in skewness and kurtosis (Fig. 5C-D) but also the nonparametric standard deviation (5B).
238 Note, in these data simulation figures Gaussian and non-Gaussian data are offset by an arbitrary amount
239 to more easily visualize their correspondence to the real data (black lines in Fig. 5).

240 To understand the practical consequences of improved growth modeling, we assembled the remainder
241 of the lichen IPM following Shriver et al. 2012. The asymptotic population growth rate λ based on Gaussian
242 growth differs from the JSU growth model by about 1% annual population growth (Table 1), in line with
243 results of Peterson et al. 2019. However, even this modest difference can lead to biased estimates of extinction
244 risk from the Gaussian model, particularly over longer time horizons (Fig. 6). We also explored differences in
245 other life history metrics (Table 1) using functions from Hernández *et al.* (2024). For example, the JSU growth
246 model predicts values for mean lifespan, mean lifetime reproductive success, and generation time that are 15–
247 25% lower than the Gaussian growth model. In this case study, properly modeling non-normal size transitions
248 – which was easy to do with a few extra lines of code – can have important effects on ecological inferences.

249 One could argue that this example was a convenient “straw man” to disqualify Gaussian growth,
250 because it was recognized by the original and subsequent analysts that size transitions are strongly skewed
251 (Peterson *et al.*, 2019; Shriver *et al.*, 2012). In all remaining case studies, including those in the Supporting
252 Information, we re-examine growth data that were modeled as Gaussian in the original published analysis.

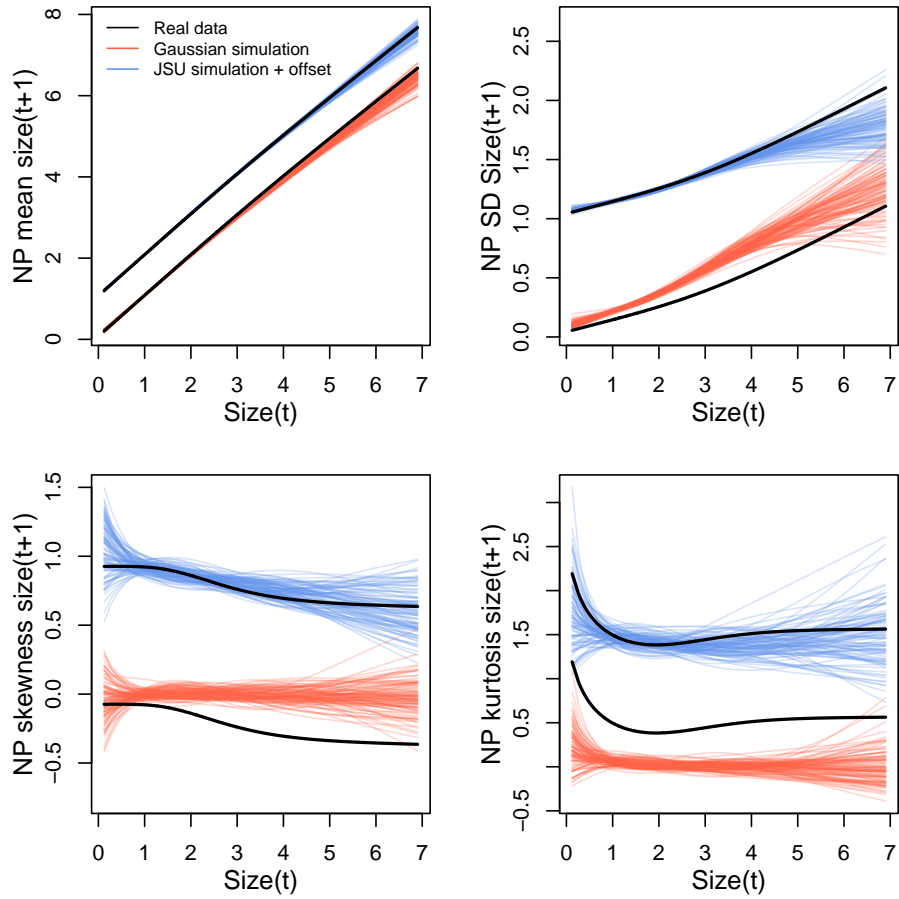


Figure 5: Comparisons among real lichen data and data simulated from Gaussian and JSU growth models for NP mean, NP standard deviation, NP skewness, and NP excess kurtosis of future size conditional on current size. Colored lines show 100 simulated data sets from the fitted Gaussian (red) or JSU (blue) growth models. Thick black line shows the real data. Gaussian and JSU data are offset by one unit and the real data line is duplicated with a one-unit offset for ease of visualization. Figure made by script `Vuplicida_IPMs.R`.

253 5 Case study: tree cholla cactus, *Cylindriopuntia imbricata*

254 The next case study, focused on the tree cholla cactus *Cylindriopuntia imbricata* at the Sevilleta Long-Term
 255 Ecological Research site in central New Mexico, adds a new feature to the simple size-dependent regressions
 256 in the previous study: random effects associated with temporal (year) and spatial (plot) environmental
 257 heterogeneity. This long-term study was initiated in 2004 and different subsets of the data have been analyzed
 258 in various IPM studies, all using Gaussian growth kernels (Compagnoni *et al.*, 2016; Czachura & Miller, 2020;
 259 Elderd & Miller, 2016; Miller *et al.*, 2009; Ohm & Miller, 2014). In fact, Elderd and Miller 2016 presented

Table 1: Life history attributes derived from IPM kernels that included Gaussian or “improved” growth sub-models for five case studies. The improved distributions were JSU (lichen, creosote), SHASH (cactus, pike), and skewed t (orchid). Pike and creosote case studies are presented in the Supporting Information. Table can be reproduced from script `crossspp_growth.R`.

Species	Growth model	λ	Lifespan	Lifetime reproductive output	Age at reproduction	Generation time
Lichen (<i>Vulpicida pinastri</i>)	Gaussian	1.001	6.443	1.031	5.588	33.869
	Improved	0.992	5.395	0.773	5.39	29.051
Cactus (<i>Cylindriopunia imbricata</i>)	Gaussian	0.994	2.003	0.03	18.959	189.41
	Improved	0.993	2.002	0.019	21.676	179.474
Orchid (<i>Orchis purpurea</i>)	Gaussian	1.091	1.081	20.009	5.064	104.125
	Improved	1.09	1.079	19.378	5.027	100.753
Pike (<i>Esox Lucius</i>)	Gaussian	1.616	1.051	0.447	1.241	4.963
	Improved	1.617	1.049	0.369	1.221	4.94
Creosote (<i>Larrea tridentata</i>)	Gaussian	1.039	21651.948	1998.486	29.338	241517.676
	Improved	1.04	19613.824	1814.89	31.668	215330.883

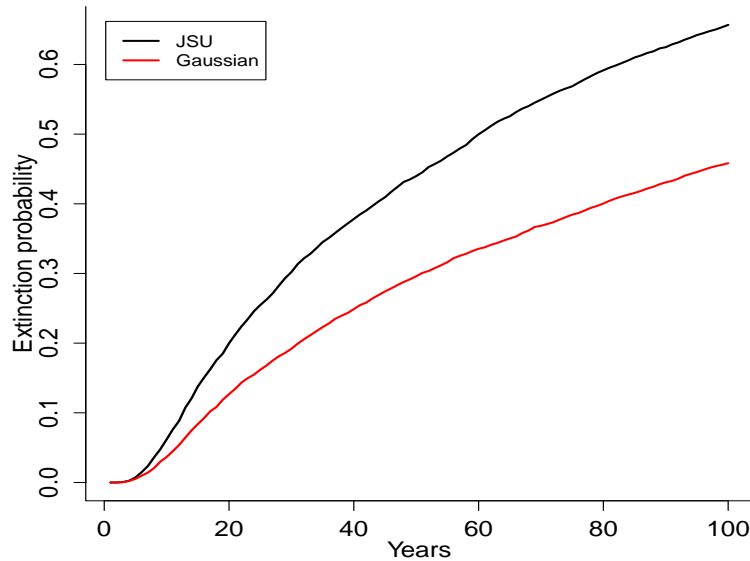


Figure 6: Extinction risk estimated from individual-based simulation of IPMs based on Gaussian and Johnson’s S-U (JSU) growth distributions. Figure made by script `Vuplicida_IPMs.R`.

- 260 a Gaussian growth model as an example of a well fit growth function, based on an overall distribution of
 261 residuals that appeared Gaussian and posterior predictive checks (PPCs) of a Bayesian model that suggested
 262 consistency between the real data and data simulated from the fitted model (Fig. 4 in (Elderd & Miller,

263 2016)). While PPCs and the associated “Bayesian P-value” are popular diagnostic tools, they are often too
264 conservative (Conn *et al.*, 2018; Zhang, 2014), failing to reject marginally bad models even though they are
265 very effective in rejecting terrible models. The choice of discrepancy function (the statistic used to compare
266 real and simulated data) can also be limiting: in our previous work, we used a discrepancy function focused
267 on variance (the sum of squared residuals), creating a blind spot for poor modeling of higher moments.

268 The data includes 4844 size transition observations from 929 individuals spanning 13 transition years
269 (2004–2018) and 11 spatial replicates (three spatial blocks in years 2004–2008 and eight 30m-by-30m plots
270 in years 2009–2018). The data are provided in Miller (2020). Following previous studies, we quantified
271 size as the natural logarithm of plant volume (cm^3), derived from height and width measurements.

272 We begin growth modeling, as above, with a generalized additive model with the mean and standard
273 deviation of size in year $t + 1$ modeled as smooth function of size in year t , with random intercepts for
274 year and plot and assuming normally-distributed residuals:

```
275 # t0 and t1 are initial and final log(volume), respectively  
276 fitGAU <- gam(list(t1 ~ s(t0,k=4) + s(plot,bs="re") + s(year,bs="re"),  
277 ~ s(t0,k=6)), data=caactus, family=gaulss())
```

278 Note that here we fitted the standard deviation function with $k=6$ basis functions rather than our default
279 of $k = 4$ because, in a preliminary analysis, we found a moderate variance trend in the standardized
280 residuals using $k=4$. With $k=6$, spline regression detected essentially no trend in the mean of the resulting
281 standardized residuals, and only a small amount of variation in the variance (Fig. 4C,D).

282 The growth variance is estimated to peak at small to medium sizes (Fig. 3C). The standardized
283 residuals show clear signals of negative skew and positive excess kurtosis across most of the size distribution,
284 but strongest in the middle (Fig. 3D). We therefore need a distribution family allowing negative skew and
285 positive excess kurtosis, both of which may be negligible at some sizes. We first tried Johnson’s S_U and

286 then the skewed t distributions, which provided some improvements but there were still visible discrepancies
287 between simulated and real data. Through repeated trial and error we arrived at the SHASH distribution,
288 which allows a greater range of kurtosis for a given amount of skew, and vice versa (Jones & Pewsey (2009);
289 Supporting Information S.1). This flexibility proved necessary to generate simulated data that compared
290 favorably to the real data. Furthermore, SHASH is available as an **mgcv** family, allowing for flexible
291 size-dependence in skewness and kurtosis without having to select specific size-dependent functions.

292 Here, the first argument to `gam()` is now a four-element list specifying the linear predictors for
293 the four parameters of the SHASH distribution.

```
294 fit_shash <- gam(list(t1 ~ s(t0,k=4) +  
295   s(plot,bs="re") + s(year_t,bs="re"), # location  
296   ~ s(t0,k=4), # log-scale  
297   ~ s(t0,k=4), # skewness  
298   ~ s(t0,k=4)), # log-kurtosis  
299   data = cactus, family = shash,optimizer = "efs")
```

300 Data simulated from the SHASH model compared favorably to the real data (Fig. 11). Similar to the lichen
301 case study, we see that correctly modeling skewness and kurtosis improved estimation of the nonparametric
302 mean and standard deviation (Fig. 11A,B), yielding a growth model that is truer to the data.

303 We next explored how improved growth modeling influenced IPM results. The λ values predicted
304 by Gaussian and SHASH growth functions, corresponding to the average plot and year, were nearly
305 identical (Table 1) but we could also leverage structure of the study design to quantify demographic
306 variance associated with temporal and spatial heterogeneity. We used the fitted random effects from the
307 vital rate models to estimate the asymptotic growth rate for each year (λ_t), centered on the average plot,
308 and for each plot (λ_p), centered on the average year. The Gaussian growth model tended to over-estimate

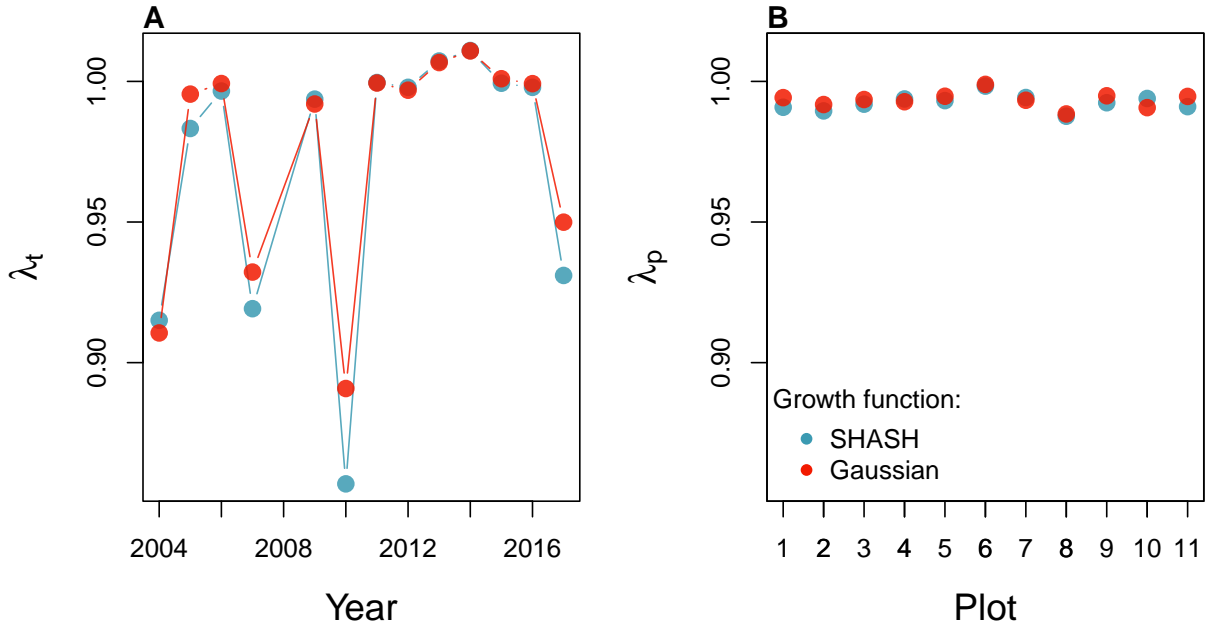


Figure 7: Temporal (A) and spatial (B) heterogeneity in fitness for the tree cholla cactus (*Cylindropuntia imbricata*) predicted by IPMs using Gaussian or SHASH growth models. Figure made by script `cactus_growth_modeling_qgam.R`.

309 λ_t , particularly in some of the harshest years (Fig. 7A), and thus under-estimated temporal variance
310 in fitness ($SD(\lambda_{t(Gaussian)}) = 0.04$, $SD(\lambda_{t(SHASH)}) = 0.048$). Plot-to-plot variation was more similar
311 ($SD(\lambda_{p(Gaussian)}) = 0.0026$, $SD(\lambda_{p(SHASH)}) = 0.0028$), although spatial variation in fitness was much lower
312 than temporal variation (Fig. 7B). The difference in temporal variance would suggest that Gaussian growth
313 modeling would lead to over-estimation of the stochastic growth rate λ_S , because temporal variance has
314 a negative effect on λ_S . However, the stochastic growth rate from the Gaussian growth model ($\lambda_S = 0.992$)
315 was only slightly higher than that of the SHASH growth model ($\lambda_S = 0.991$). This is likely because temporal
316 fluctuations in vital rates, which is where the SHASH growth model would make a difference, have a
317 weaker influence on λ_S than the temporal fluctuations in size structure that they generate (Compagnoni
318 *et al.*, 2016; Ellis & Crone, 2013). In other life history traits, the SHASH and Gaussian growth models
319 predicted nearly identical lifespans but the SHASH predicted an older age at reproduction and shorter
320 generation time (Table 1). Thus, in this case study, modeling non-Gaussian size transitions with a Gaussian
321 growth model may or may not influence IPM results depending on the target of the analysis.

322 **6 Case study: lady orchid, *Orchis purpurea***

323 Our final case study examines selection on life history strategies in the lady orchid *Orchis purpurea*. In
324 a prior study, Miller et al. 2012 analyzed how costs of reproduction (flowering or not in year t) affected
325 growth from year t to $t + 1$. The two growth kernels for flowering and non-flowering were then used in
326 an IPM to quantify the optimal flowering size that balances the benefits of waiting to flower at larger sizes
327 against the greater risk of death before flowering. The original study assumed Gaussian size transitions
328 with non-constant variance depending on initial size. Here we re-visit that analysis to derive improved
329 growth kernels. We use this case study to illustrate several new elements and challenges, including modeling
330 skewness and kurtosis as functions of expected future size.

331 The data, originated by Dr. Hans Jacquemyn, come from 368 plants in a Belgian population censused
332 annually from 2003 through 2011. Here we use data only from the “light” habitat in the original study.
333 We used the natural logarithm of total leaf area as the size variable in the IPM.

334 As a variation on software, we fitted the pilot Gaussian model using the `lmer` function in the **lme4**
335 package. We fit three candidate linear models that included fixed effects of size in year t (model 1), additive
336 effects of size and flowering status in year t (model 2), or an interaction between size and flowering (model
337 3), all including random intercepts for year. The interaction model with strongly favored ($\Delta AIC = 10.5$).
338 Unlike our previous case studies, here we have multiple fixed effects (initial size and flowering status)
339 that may influence the variance of future size. In cases such as this it is convenient to model variance as
340 a function of expected future size, rather than initial size as we did with the lichens and cacti. The expected
341 (or “fitted”) values reflect the combined influence of all fixed and random effects, and therefore implicitly
342 account for multiple sources of variation in the variance.

343 Models where error variance is a function of fitted values cannot be fitted directly with `lme4` (nor in
344 the **mgcv** functions for generalized additive models). But it can still be done with `lmer` through an iterative

345 re-weighting approach, as follows. In `lmer`, weights w_i can be used to indicate that the observations y_i
346 have error variance proportional to $1/w_i^2$. The iterative steps are as follows, and code that executes these
347 steps is in `orchid_growth_modeling.R`.

- 348 1. Fit the expected value assuming Gaussian-distributed residuals with constant variance.
- 349 2. Fit the standard deviation of the residuals as a function of the corresponding fitted value.
- 350 3. Re-fit the model, with weights equal to the inverse of the standard deviation estimated in step 2.

351 We iterated steps 2 and 3 until the root mean square change in weights was below 10^{-6} . This is not elegant,
352 but it works and converges quickly. In step 2, we modeled the log of the standard deviation (because standard
353 deviations cannot be negative) as a quadratic polynomial in the fitted mean. In exploratory analyses we found
354 that the quadratic term was necessary to fit the standard deviation. We did this for all candidate models and,
355 for a fair AIC comparison, we then re-fit all candidate models with the weights estimated from the top model.

356 The updated model selection continued to favor the size \times flowering interaction model (3), but now
357 with a weaker improvement over the next-best model ($\Delta AIC = 6.7$). The fitted mean (a function of initial
358 size and flowering status) and fitted standard deviation (a function of the fitted mean) are shown in Fig.
359 3E. Spline regression found no trend in the mean of the resulting standardized residuals, and only small
360 variation in the variance (Fig. 4E,F).

361 The best Gaussian model indicated a growth cost associated with flowering at the start of the census
362 interval and a decline in growth variance with increasing expected values (Fig. 3E). The standardized
363 residuals indicated negative skewness (10–20% difference in tail weight) and excess kurtosis (10–40% fatter
364 than Gaussian) across much of the size distribution but both negligible at large expected sizes (Fig. 3F).

365 As possible improvements, we explored the skewed t and JSU distributions, both leptokurtic
366 distributions with flexible skewness. We were happier with the skewed t , which we fit with a custom
367 likelihood function similar to the JSU growth model for the lichen data. However, rather than re-fitting

368 all parameters of the skewed t model, as we did with the lichen JSU, we built a “hybrid” likelihood function
 369 that uses the fitted mean and standard deviation from the best Gaussian model, and estimates parameters that
 370 control skewness and kurtosis as linear functions of expected future size. This is easy because the **gamlss.dist**
 371 package provides a parameterization of the skewed t in which the location parameter μ is the mean and
 372 scale parameter σ is the standard deviation (Rigby *et al.*, 2019). The hybrid likelihood looks like this:

```

 373 ## GAU_fitted and GAU_sd are mean & standard deviation from the best Gaussian.  

 374 SSTLogLik=function(pars){  

 375   dSST(log_area_t1,  

 376     mu=GAU_fitted, sigma=GAU_sd,  

 377     nu = exp(pars[1] + pars[2]*GAU_fitted),  

 378     tau = exp(pars[3] + pars[4]*GAU_fitted)+2, log=TRUE)  

 379 }  

 380 p0<-c(0,0,0,0) ## default starting parameters  

 381 SSTout=maxLik(logLik=SSTLogLik,start=p0) ## fit with maxLik

```

382 Based on diagnostics of the standardized residuals, parameters that control skewness and kurtosis are defined
 383 as linear functions of the mean (note that the τ parameter uses a $\log(x-2)$ link function). This approach
 384 relies on the robustness of fitted Gaussian models to deviations from normality, which implies that the fitted
 385 mean and variance from a Gaussian model are good approximations for the fitted mean and variance of
 386 the corresponding non-Gaussian model. If one is skeptical of this approach, it is possible to simultaneously
 387 re-fit all parameters of the skewed t . However, recall that unlike the lichen case study, the pilot Gaussian
 388 model here includes random year effects, and the expected values getting passed into dSST account for
 389 this source of variation. Estimating random effects “from scratch” with a custom likelihood model is
 390 possible (we provide guidance on doing this with a “shrinkage” approach, in Supporting Information S.2),

391 but generally should not be necessary. Instead, a key advantage of the hybrid approach is retention of
392 the fitted random effects and associated variance components, which get shuttled from the Gaussian model
393 into the non-Gaussian model without any fuss (though it was critical to use a parameterization of the skewed
394 t for which μ is the mean and σ is the standard deviation). And, if this approach does not “work”
395 (i.e., deviations from normality biased the fitted values of the Gaussian model) one would quickly find
396 out when comparing simulated with real data. In this case, size transition data simulated from this model
397 corresponded favorably to the real data, much better than the pilot Gaussian model, including improvements
398 in the standard deviation, skewness, and kurtosis of future size (Fig. 12).

399 Finally, we used the improved growth model to revisit key results of the original study. Miller et
400 al. (2012) used the orchid IPM to estimate the evolutionarily stable strategy (ESS) as the mean size at
401 flowering that maximizes lifetime reproductive success (R_0), given the constraint that flowering when
402 small reduces growth and thus elevates mortality risk. Repeating that analysis here, we found that improved
403 growth modeling has virtually no influence on predictions for optimal life history strategies (Fig. 8). ESS
404 flowering sizes were nearly identical between IPMs with Gaussian vs skewed t growth models, and both
405 aligned well with the observed mean flowering size (dashed vertical line in Fig. 8). Similarly, there were
406 very small differences between growth functions in other metrics of orchid life history (Table 1).

407 7 Discussion

408 Much of the appeal of IPMs has stemmed from their embrace of continuous size structure through regression-
409 based approaches, and the potentially complex fixed- and random-effect structures that those approaches allow.
410 Using familiar statistical tools and with relatively few parameters to estimate, IPM users can incorporate
411 important sources of variation in demography and interrogate their influence on ecological and evolutionary
412 dynamics. With this opportunity comes the burden of getting it right: an IPM is only as good as the statistical
413 sub-models for the underlying data. The growth sub-model is the trickiest part because it defines a distribu-

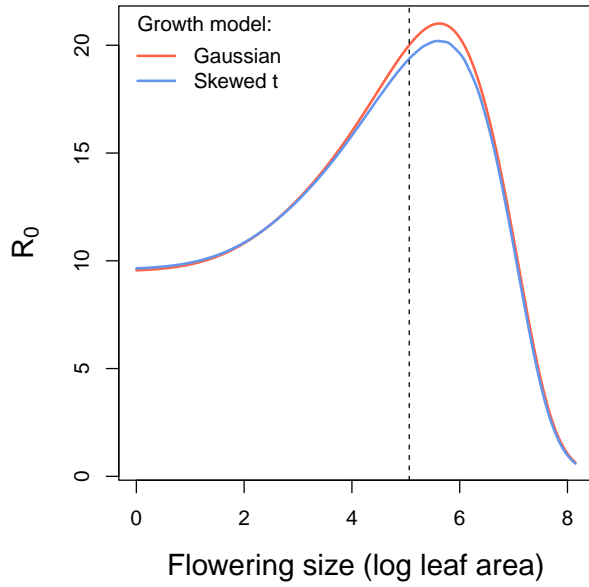


Figure 8: Orchid life history results from IPMs using Gaussian or skewed t growth models. Lifetime reproductive success (R_0) is shown as a function of mean size of flowering. Dashed vertical line shows the observed mean flowering size.

414 tion of future size conditional on current size. Distributions have many properties – “moments” – and a good
 415 growth model should recapitulate the properties of real size transitions. The default assumption of Normally
 416 distributed size transitions, employed overwhelmingly across 20+ years of IPM studies, is an arbitrary histori-
 417 cal precedent. In our case studies and, we suspect, more broadly, skewness and excess kurtosis were common
 418 features of size transitions. Our most important message is that the assumption of normally-distributed size
 419 transitions can easily be abandoned, and a more inquisitive process of growth modeling should take its place.
 420

420 We have attempted to lay out what that process should look like, emphasizing visual diagnostics
 421 to characterize how data deviate from Gaussian. One implication of relying on visual diagnostics is that
 422 goodness of fit is in the eye of the beholder. This empowers IPM users to make informed choices, but it is not
 423 very prescriptive; we have not suggested any hard rules for choosing among distributions, only that a good
 424 growth model should generate data that look like the real thing. Alternatively, model selection could be used
 425 to identify best-fitting growth distributions and best-fitting functions for higher moments. However, model

426 selection among growth distributions with 3-5 parameters, each of which may be functions of multiple state
427 variables or fitted values, can quickly explode in complexity, and we are not convinced it is worth the trouble.

428 Our work follows the important contribution of Peterson et al. 2019, who were similarly motivated
429 by inadequacy of the Gaussian model but arrived at different recommendations. These authors developed
430 a creative approach in which size data are transformed onto a [0,1] scale and size transitions on that scale
431 are modeled using beta regression. The beta distribution can accommodate positive, negative, or zero skew,
432 potentially varying with size, so the Peterson et al. approach is a flexible option for skewed growth data.
433 However, beta regression also has some limitations: common beta regression packages do not fit random
434 effects (e.g., **betareg** (Cribari-Neto & Zeileis, 2010)) or do not do so reliably (in our experience **gamlss**
435 regressions with random effects are numerically unstable); and the two-parameter beta distribution does
436 not allow skewness and kurtosis to be fitted independently. Additionally, the initial transformation onto
437 [0,1] scale requires estimating extreme quantiles of the growth distribution (e.g., 0.01 and 0.99) as a function
438 of initial size. In our experience those quantile estimates can be very sensitive to how size-dependence is
439 modeled, and model selection is challenging for extreme quantiles where data are (by definition) very sparse.
440 Rather than picking one distribution as a new default, users can leverage the vast arsenal of continuous
441 probability distributions – all at one’s fingertips with a few lines of code – so that the data and their particular
442 deviations from normality can guide the choice of a better distribution.

443 In all of our case studies, non-Gaussian growth models always yielded more satisfying fits to size
444 transition data than the Gaussian models published in those papers. However, to our relief, none of these
445 re-analyses yielded a “gotcha” result that overturned results of the original study. In this small sampling
446 of case studies, improved growth modeling had weak to modest effects on IPM results (Table 1), similar in
447 magnitude to the results of Peterson *et al.* (2019). For some case studies, one might argue that non-Gaussian
448 modeling was not worth the trouble – only it was almost no trouble at all, and we could not have known
449 whether or not a non-Gaussian model would have made a difference before fitting it.

450 We caution against taking too much comfort in weak effects of “improved” growth modeling; in
451 other scenarios the choice of the growth distribution could be more consequential. It is worth noting that
452 most of our case studies focused on perennial life histories (perennial plants and lichens) characterized
453 by relatively slow growth, heavy losses during recruitment, and high survival once established, and these
454 species all had mean lifespans between one and six years and generation times on the order of decades. Life
455 histories such as these may be relatively robust to subtle features of the growth kernel. In the Supporting
456 Information we present three additional case studies that broaden our life history coverage, including pike
457 (*Esox lucius*), a fish with a generation time of four to five years and creosotebush (*Larrea tridentata*), a
458 desert shrub that is virtually immortal once established with a generation time exceeding 200,000 years.
459 Life history metrics from the “fast” fish population were no more sensitive to improved growth modeling
460 than those of the perennial plants and lichens, while the creosotebush generation time differed by >25,000
461 years between Gaussian and improved growth models (Table 1). More systematic comparative analyses
462 may provide insight into which types of species and life histories are more likely to exhibit strong skewness
463 and kurtosis, and which demographic quantities are more or less sensitive to these features of size transition.

464 Our case studies illustrate a diversity of software packages and computational approaches, to reflect
465 the diversity of preferences and habits that the community of IPM analysts bring to their own problems.
466 We like spline generalized additive models (gams) for their flexibility and for **mgcv**’s numerous options
467 for distribution families and overall speed and reliability. However, there are some applications for which
468 classical parametric regression would be preferable because the coefficients carry biological meaning. For
469 example, regression coefficients may be targets of natural selection (Rees & Ellner, 2016) and may combine
470 to influence traits of interest such as the expected size at flowering (e.g. in Fig. 8A), a function of the intercept
471 and slope of the size-dependent flowering function (Metcalf *et al.*, 2003). Some potentially useful distributions
472 are not available in linear modeling software packages, but that should not be a barrier to their use: as in
473 several of our case studies, custom likelihood functions allow non-Gaussian models without sacrificing the

474 complex, multi-level features that one might be accustomed to fitting in **lme4**, for example. Bayesian analysis
475 may further broaden the options for non-Gaussian candidate distributions and may help estimate hard-to-fit
476 parameters through the brute force of sampling algorithms. Bayesian analysis also provides a natural way
477 to propagate uncertainty from vital rate sub-models to full model predictions (Elderd & Miller, 2016).

478 From the outset there have been concerns about “how well these methods [IPM growth kernels] can
479 deal with different patterns of growth, stasis, and shrinkage” (Morris & Doak, 2002, p. 200), compared to
480 “binning” methods that use observed transition frequencies between user-defined size classes as the transition
481 probabilities in a (possibly large) matrix model (Doak *et al.*, 2021). The non-Gaussian models that we have
482 considered here are not a panacea. For example, none of them allow bimodal growth, such as might occur if
483 herbivore- or pathogen-attached individuals experience rapid tissue loss. When the shape of the growth distri-
484 bution is nearly the same for all initial sizes, a nonparametric IPM growth kernel can be defined from a kernel
485 density estimate for scaled residuals (Ellner *et al.*, 2016, p. 288). Outside that special situation, nonparametric
486 approaches require choosing multiple smoothing parameters, which is very challenging. We are currently
487 exploring whether “targeted learning” approaches developed for causal inference (van der Laan & Rose,
488 2011) can be used to circumvent smoothing parameter selection. Targeted learning starts with a pilot model
489 and updates it iteratively to achieve unbiased estimates and valid confidence intervals for a particular “target”
490 quantity, such as λ or mean lifespan. Preliminary results suggest that targeted learning with a deliberately
491 under-smoothed pilot model works well for complex growth patterns (G. Hooker and Y. Zhou, *personal com-*
492 *munication*). But nonparametric methods are data-hungry, so when departures from Gaussian are quantitative
493 rather than qualitative, parametric modeling as developed here will make more efficient use of limited data.

494 Conclusion

495 Gaussian-distributed size transitions are probably the exception in nature, not the rule, yet two decades
496 of IPM studies have relied overwhelmingly on Gaussian growth models. Using tools not available when

497 IPMs were first developed, it should often be possible now to make major improvements over a Gaussian
498 model, without worrying about finding the “best” alternative. By generating predicted size transitions
499 that are truer to the data, IPM analysts can narrow the gap between model and nature.

500 **Acknowledgements:** This research was supported by US NSF grants DEB-1933497 to SPE and
501 DEB-1754468, 2208857, and 2225027 to TEXM. The Sevilleta LTER (source of the cactus and creosote
502 case studies) is supported by DEB-1655499 and DEB-1748133. Giles Hooker gave us the very good idea
503 to use quantile regression instead of binning to estimate trends in skewness and kurtosis. Ali Campbell
504 and Jacob Moutouama provided helpful discussion and comments on the manuscript.

505 **Authorship statement:** All authors discussed all aspects of the research and contributed to developing
506 methods, analyzing data, and writing and revising the paper.

507 **Conflict of interest statement:** The authors have none to declare.

508 Literature Cited

- 509 Adler, P.B., Kleinhesselink, A., Hooker, G., Taylor, J.B., Teller, B. & Ellner, S.P. (2019) Data from: Weak
510 interspecific interactions in a sagebrush steppe? Conflicting evidence from observations and experiments.
511 Dryad Data set. <https://doi.org/10.5061/dryad.96dn293>.
- 512 Anscombe, F.J. & Glynn, W.J. (1983) Distribution of the kurtosis statistic b_2 for normal samples. *Biometrika*
513 **70**, 227–234.
- 514 Bates, D., Mächler, M., Bolker, B. & Walker, S. (2015) Fitting linear mixed-effects models using lme4.
515 *Journal of Statistical Software* **67**, 1–48.

- 516 Compagnoni, A., Bibian, A.J., Ochocki, B.M., Rogers, H.S., Schultz, E.L., Sneck, M.E., Elderd, B.D.,
- 517 Iler, A.M., Inouye, D.W., Jacquemyn, H. *et al.* (2016) The effect of demographic correlations on the
- 518 stochastic population dynamics of perennial plants. *Ecological Monographs* **86**, 480–494.
- 519 Conn, P.B., Johnson, D.S., Williams, P.J., Melin, S.R. & Hooten, M.B. (2018) A guide to Bayesian model
- 520 checking for ecologists. *Ecological Monographs* **88**, 526–542.
- 521 Cooch, E.G. & White, G.C. (2020, accessed 5/17/2020) *Program MARK - a 'gentle introduction'*. phidot.org.
- 522 Coulson, T. (2012) Integral projections models, their construction and use in posing hypotheses in ecology.
- 523 *Oikos* **121**, 1337–1350.
- 524 Cribari-Neto, F. & Zeileis, A. (2010) Beta regression in R. *Journal of statistical software* **34**, 1–24.
- 525 Crone, E.E. (2016) Contrasting effects of spatial heterogeneity and environmental stochasticity on population
- 526 dynamics of a perennial wildflower. *Journal of Ecology* **104**, 281–291.
- 527 Czachura, K. & Miller, T.E. (2020) Demographic back-casting reveals that subtle dimensions of climate
- 528 change have strong effects on population viability. *Journal of Ecology* **108**, 2557–2570.
- 529 D'Agostino, R.B. (1970) Transformation to normality of the null distribution of g_1 . *Biometrika* **57**, 679–681.
- 530 Davis, C. (2015) *sgt: Skewed Generalized T Distribution Tree*. R package version 2.0.
- 531 Doak, D.F., Waddle, E., Langendorf, R.E., Louthan, A.M., Isabelle Chardon, N., Dibner, R.R., Keinath,
- 532 D.A., Lombardi, E., Steenbock, C., Shriver, R.K., Linares, C., Begoña Garcia, M., Funk, W.C., Fitzpatrick,
- 533 S.W., Morris, W.F. & DeMarche, M.L. (2021) A critical comparison of integral projection and matrix
- 534 projection models for demographic analysis. *Ecological Monographs* **91**, e01447.
- 535 Easterling, M.R., Ellner, S.P. & Dixon, P.M. (2000) Size-specific sensitivity: applying a new structured
- 536 population model. *Ecology* **81**, 694–708.

- 537 Elderd, B.D. & Miller, T.E. (2016) Quantifying demographic uncertainty: Bayesian methods for integral
538 projection models. *Ecological Monographs* **86**, 125–144.
- 539 Ellis, M.M. & Crone, E.E. (2013) The role of transient dynamics in stochastic population growth for nine
540 perennial plants. *Ecology* **94**, 1681–1686.
- 541 Ellner, S.P., Adler, P.B., Childs, D.Z., Hooker, G., Miller, T.E. & Rees, M. (2022) A critical comparison of
542 integral projection and matrix projection models for demographic analysis: Comment. *Ecology* **103**, e3605.
- 543 Ellner, S.P., Childs, D.Z. & Rees, M. (2016) *Data-driven Modeling of Structured Populations: A Practical
544 Guide to the Integral Projection Model*. Springer, New York.
- 545 Fasiolo, M., Wood, S.N., Zaffran, M., Nedellec, R. & Goude, Y. (2020) qgam: Bayesian non-parametric
546 quantile regression modelling in R. *arXiv preprint arXiv:2007.03303* .
- 547 Gu, C. (2013) *Smoothing Spline ANOVA Models*. Springer Science+Business Media, New York, 2 edn.
- 548 Hadfield, J.D. *et al.* (2010) MCMC methods for multi-response generalized linear mixed models: the
549 mcmcglmm r package. *Journal of Statistical Software* **33**, 1–22.
- 550 Héault, B., Bachelot, B., Poorter, L., Rossi, V., Bongers, F., Chave, J., Paine, C.T., Wagner, F. & Baraloto,
551 C. (2011) Functional traits shape ontogenetic growth trajectories of rain forest tree species. *Journal
552 of ecology* **99**, 1431–1440.
- 553 Hernández, C.M., Ellner, S.P., Snyder, R.E. & Hooker, G. (2024) The natural history of luck: A synthesis
554 study of structured population models. *Ecology Letters* pp. 0 – 1.
- 555 Komsta, L. & Novomestky, F. (2015) moments: Moments, cumulants, skewness, kurtosis and related tests.
556 *R package version 0.14.1*.

- 557 Louthan, A.M., Keighron, M., Kiekebusch, E., Cayton, H., Terando, A. & Morris, W.F. (2022) Climate
558 change weakens the impact of disturbance interval on the growth rate of natural populations of venus
559 flytrap. *Ecological Monographs* **92**, e1528.
- 560 McGillivray, H. (1986) Skewness and asymmetry: measures and orderings. *Annals of Statistics* **14**, 994–1011.
- 561 Metcalf, C.J.E., Ellner, S.P., Childs, D.Z., Salguero-Gómez, R., Merow, C., McMahon, S.M., Jongejans,
562 E. & Rees, M. (2015) Statistical modelling of annual variation for inference on stochastic population
563 dynamics using Integral Projection Models. *Methods in Ecology and Evolution* **6**, 1007–1017.
- 564 Metcalf, J.C., Rose, K.E. & Rees, M. (2003) Evolutionary demography of monocarpic perennials. *Trends
565 in Ecology & Evolution* **18**, 471–480.
- 566 Miller, T.E. (2020) Long-term study of tree cholla demography in the los pinos mountains, sevilleta national
567 wildlife refuge. <https://doi.org/10.6073/pasta/dd06df3f950afe4a4642306182237d13>.
- 568 Miller, T.E., Louda, S.M., Rose, K.A. & Eckberg, J.O. (2009) Impacts of insect herbivory on cactus
569 population dynamics: experimental demography across an environmental gradient. *Ecological
570 Monographs* **79**, 155–172.
- 571 Miller, T.E., Williams, J.L., Jongejans, E., Brys, R. & Jacquemyn, H. (2012) Evolutionary demography
572 of iteroparous plants: incorporating non-lethal costs of reproduction into integral projection models.
573 *Proceedings of the Royal Society B: Biological Sciences* **279**, 2831–2840.
- 574 Morris, W.F. & Doak, D.F. (2002) *Quantitative Conservation Biology: Theory and Practice of Population
575 Viability Analysis*. Sinauer Associates, Sunderland, Mass.
- 576 Ohm, J.R. & Miller, T.E. (2014) Balancing anti-herbivore benefits and anti-pollinator costs of defensive
577 mutualists. *Ecology* **95**, 2924–2935.

- 578 Ozgul, A., Childs, D.Z., Oli, M.K., Armitage, K.B., Blumstein, D.T., Olson, L.E., Tuljapurkar, S. & Coulson,
579 T. (2010) Coupled dynamics of body mass and population growth in response to environmental change.
580 *Nature* **466**, 482–485.
- 581 Peterson, M.L., Morris, W., Linares, C. & Doak, D. (2019) Improving structured population models with
582 more realistic representations of non-normal growth. *Methods in Ecology and Evolution* **10**, 1431–1444.
- 583 Plard, F., Schindler, S., Arlettaz, R. & Schaub, M. (2018) Sex-specific heterogeneity in fixed morphological
584 traits influences individual fitness in a monogamous bird population. *The American Naturalist* **191**,
585 106–119.
- 586 R Core Team (2022) *R: A Language and Environment for Statistical Computing*. R Foundation for Statistical
587 Computing, Vienna, Austria.
- 588 Rees, M., Childs, D.Z. & Ellner, S.P. (2014) Building integral projection models: a user's guide. *Journal
589 of Animal Ecology* **83**, 528–545.
- 590 Rees, M. & Ellner, S.P. (2016) Evolving integral projection models: evolutionary demography meets
591 eco-evolutionary dynamics. *Methods in Ecology and Evolution* **7**, 157–170.
- 592 Rigby, R.A., Stasinopoulos, M.D., Heller, G.Z. & De Bastiani, F. (2019) *Distributions for modeling location,
593 scale, and shape: Using GAMLS in R*. CRC press.
- 594 Salguero-Gómez, R. & Casper, B.B. (2010) Keeping plant shrinkage in the demographic loop. *Journal
595 of Ecology* **98**, 312–323.
- 596 Schielzeth, H., Dingemanse, N.J., Nakagawa, S., Westneat, D.F., Allegue, H., Teplitsky, C., Réale, D.,
597 Dochtermann, N.A., Garamszegi, L.Z. & Araya-Ajoy, Y.G. (2020) Robustness of linear mixed-effects
598 models to violations of distributional assumptions. *Methods in ecology and evolution* **11**, 1141–1152.

- 599 Shriver, R.K., Cutler, K. & Doak, D.F. (2012) Comparative demography of an epiphytic lichen: support
600 for general life history patterns and solutions to common problems in demographic parameter estimation.
601 *Oecologia* **170**, 137–146.
- 602 Stasinopoulos, D.M., Rigby, R.A. *et al.* (2007) Generalized additive models for location scale and shape
603 (GAMLSS) in r. *Journal of Statistical Software* **23**, 1–46.
- 604 Stubberud, M.W., Vindenes, Y., Vøllestad, L.A., Winfield, I.J., Stenseth, N.C. & Langangen, Ø. (2019)
605 Effects of size-and sex-selective harvesting: An integral projection model approach. *Ecology and
606 Evolution* **9**, 12556–12570.
- 607 van der Laan, M.J. & Rose, S. (2011) *Targeted Learning: Causal Inference for Observational and
608 Experimental Data*. Springer Science and Business Media.
- 609 Wan, X., Wang, W., Liu, J. & Tong, T. (2014) Estimating the sample mean and standard deviation from
610 the sample size, median, range and/or interquartile range. *BMC medical research methodology* **14**, 1–13.
- 611 Williams, J.L., Miller, T.E. & Ellner, S.P. (2012) Avoiding unintentional eviction from integral projection
612 models. *Ecology* **93**, 2008–2014.
- 613 Wood, S. (2017) *Generalized Additive Models: An Introduction with R*. Chapman and Hall/CRC, 2 edn.
- 614 Zhang, J.L. (2014) Comparative investigation of three Bayesian *p* values. *Computational Statistics & Data
615 Analysis* **79**, 277–291.